

## Studies on Selenium-Organic Polymer Interfaces

Y. S. CHIANG\* and S. W. ING, JR., *Research Laboratories, Xerox Corporation, Webster, New York 14580*

### Synopsis

Interfaces of evaporated vitreous selenium and various organic polymeric resins of both the thermosetting and thermoplastic type have been studied by ultra-thin sectioning and transmission electron microscopy techniques. Epoxy, phenoxy, polyamide, butadiene-styrene copolymer, vinyl-toluene-butadiene copolymer, styrene-acrylate copolymer, and vinyltoluene-acrylate copolymer resins as well as polyethylene are among those organic polymers studied. Interfaces prepared by vacuum evaporation of selenium onto the various substrates and under varying processing conditions were examined. Intermixing and interdiffusion of the inorganic and organic polymers in the interfacial region were observed in certain cases when selenium was evaporated onto incompletely cured epoxy or lower viscosity polymers. These occurrences were found to contribute significantly to the mechanical strength of the assembly. Electrical properties of certain specific systems have also been investigated.

### INTRODUCTION

Adhesion of polymeric materials has been rather extensively studied by various techniques<sup>1</sup> in the past decade; most of these studies have dealt with organic systems. Several theories have been proposed on the mechanism of adhesion of polymers.<sup>1</sup> None of the theories are sufficiently universal, primarily because of the large variations in the chemical and physical nature of the systems studied, but also because of the lack of an ideal testing method for a precise determination of the interfacial forces.

Little attention, if any, has been given to the study of the adhesion of polymers evaporated onto another material. We have studied such a system by evaporating under vacuum an inorganic polymer, selenium, onto a number of organic polymeric substrates. Selenium is a photoconductor and is being used extensively in electrophotography.<sup>2</sup> A proper understanding of the resulting adhesion of the two materials requires both an understanding of the behavior of the molecular layers which first condense on the substrate and an understanding of the nature of the substrate surface and the interactions thereof. Ultramicrotomy, i.e., ultra-thin sectioning, coupled with high resolution electron microscopy and diffraction measurements provides an ideal method for studying the interfacial structures and, thus, provides some insight into the resulting mechanical bonding characteristics.

Epoxy resins (both unmodified and modified bisphenol-A type resin),

\* Present Address: RCA Laboratories, Princeton, N.J. 08540

phenoxy resin, polyamide resin, butadiene-styrene copolymer, vinyltoluene-butadiene copolymer, styrene-acrylate copolymer, vinyltoluene-acrylate copolymer, and polyethylene are among the various polymeric organic substrates studied. Both the thermosetting and thermoplastic type of polymeric materials have been included.

### EXPERIMENTAL PROCEDURE

The Se-epoxy-Al system used in our experiments was fabricated in the following way. The organic substrate was prepared by first depositing it onto a mechanical support (usually a thin aluminum foil) before depositing the selenium. The aluminum was degreased ultrasonically in trichloroethylene and/or etched chemically. The epoxy was then spread on the aluminum by using a knife edge. For an extremely thin layer of epoxy, the metal substrate was dipped into a 10% solution of methyl ethyl ketone and resin-curing agent mixture. Evaporation of the highly volatile solvent (methyl ethyl ketone) left an extremely thin but uniform film of adhesive on the metal. The resin was cured under controlled conditions, and at a known point in the curing process, selenium (99.999%) was evaporated onto the epoxy surface under a vacuum of about  $10^{-5}$  torr. The substrate was held at  $50^{\circ}\text{C}$ , and the deposition rate of selenium was approximately 15–20  $\mu/\text{hr}$ . After the selenium was deposited, the epoxy was allowed to cure completely before making any measurement of the composite system.

The other Se-organic resin-Al systems were fabricated by first depositing the resin onto the Al foil by dipping the metal substrate into a dilute solution of the resin in an organic solvent. The solvent for the phenoxy resin was a 1:1 mixture of acetone and toluene, and that for polyamide resin was a 1:1 mixture of isopropanol and toluene. The solvent for the copolymer resins and polyethylene was xylene. After a thin coating of the resin had been produced by evaporation of the solvent, the substrate was transferred to the vacuum evaporator. Selenium was deposited onto these organic resin-Al substrates under conditions identical to those of the Se-epoxy-Al systems, i.e.,  $50^{\circ}\text{C}$  substrate temperature and a vacuum of about  $10^{-5}$  torr.

Samples fabricated as described above were embedded in a rigid epoxy matrix and then sectioned by a Leitz ultramicrotome by use of a diamond knife. Thin cross sections, ranging from a few hundred to 2000 Å in thickness, were obtained.

The interface structures of these sections were studied by transmission electron microscopy with the use of a Philips Model EM 200 electron microscope. The samples were subjected to various degrees of flexing, tensile stress, or stripping by adhesive tapes for mechanical fracture studies. The fractured surfaces were then examined through thin cross sections of the embedded sample and by replication of the surface topology by using the electron microscope. The characteristic electrical properties of the composite system were determined by xerographic measurements, or, more precisely, by measurement of the photodischarge of the capacitively

charged photoconductor.<sup>3</sup> A schematic of the photoresponse measurement apparatus is shown in Figure 1.

## EXPERIMENTAL RESULTS

### Selenium-Epoxy System

#### *Interface Structure and Mechanical Fracture Studies*

The interfacial structure of a selenium film evaporated onto an "incompletely cured" epoxy resin (70 parts Ciba Araldite 6020 epoxy resin, 30 parts Lancast A curing agent) on aluminum is shown as Figure 2. The dark area of Figure 2 is selenium; the lighter part is epoxy. The dark stripes appearing in the epoxy region is caused by wrinkles of the thin epoxy film. The evaporation of the selenium shown in Figure 2 began after curing the epoxy resin at 50°C for 130 min under vacuum. The temperature of the substrate was maintained at 50°C while depositing the selenium and a total cure of 7 hr at (50°C) was given to the epoxy in processing the sample. Some irregularities at the Se-epoxy interface can be seen in Figure 2 plus a few occlusions of selenium in epoxy and vice versa.

The system described above exhibited excellent bonding between selenium and the substrate and did not fail when subjected to a severe flexing or stripping test.

On the other hand, selenium deposited under identical conditions but on a "well cured" epoxy resin of the same composition did not withstand the same flexing and stripping test. The selenium layer flaked or peeled off easily. The well cured epoxy resin was cured at 50°C in a temperature-controlled oven for 16 hr. The interface of the selenium and the well cured epoxy resin is illustrated in Figure 3. A distinctly different structure than that of Figure 2 is noted.

To better understand the observed interface structure of the Se-epoxy system, we investigated four controllable parameters: (1) variation of curing agent, (2) ratio of curing agent to resin, (3) curing time before commencing evaporation of selenium, and (4) the resin itself. Each of these parameters in fabricating the Se-incompletely cured epoxy system

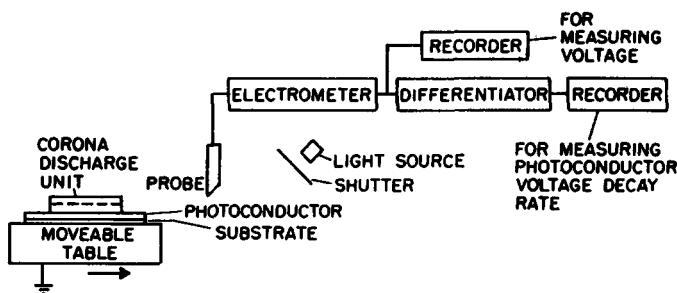


Fig. 1. Photoresponse measurement apparatus.

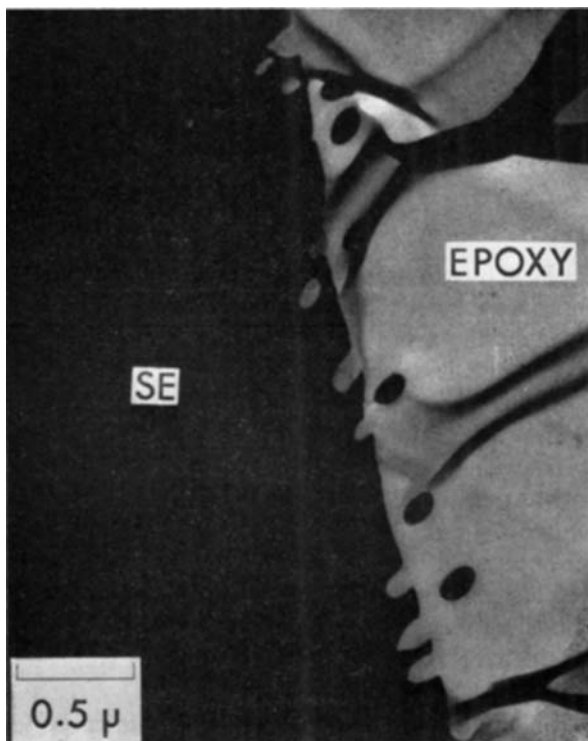


Fig. 2. Transmission electron micrograph of ultrathin sections of Se-epoxy interface (system A).

will be discussed in the following sections. In each of the experiments, only the specifically mentioned parameter is altered and all other conditions remain the same.

**Variation of Curing Agent.** The Lancast A was replaced by a slower acting curing agent, e.g., nadic anhydride, in the epoxy resin mixtures. This slower acting curing agent gave equally good bonding characteristics when used in a system where the selenium was evaporated onto incompletely cured epoxy. However, a different interface structure was noted, and a comparison with the structure of Figure 2 showed a more irregular interface and deeper epoxy penetration into selenium.

**Ratio of Curing Agent to Resin.** A variation in the ratio of curing agent to resin produced equally dramatic results. Figure 4 is an illustration of the effect of reducing the curing agent from 30 parts to 20 parts (20 parts Lancast A and 80 parts Araldite 6020 epoxy resin). A large amount of selenium occlusion in epoxy is observed. The regions between and around the selenium particles in Figure 4 are shadowy, indicating dilute dispersions of selenium in the epoxy. A much higher magnification of a shadowy region shows the bulk selenium and the epoxy to be separated by an irregular layer of selenium dispersed in epoxy. The boundaries between the selenium, dispersion layer, and epoxy are well defined, but there is

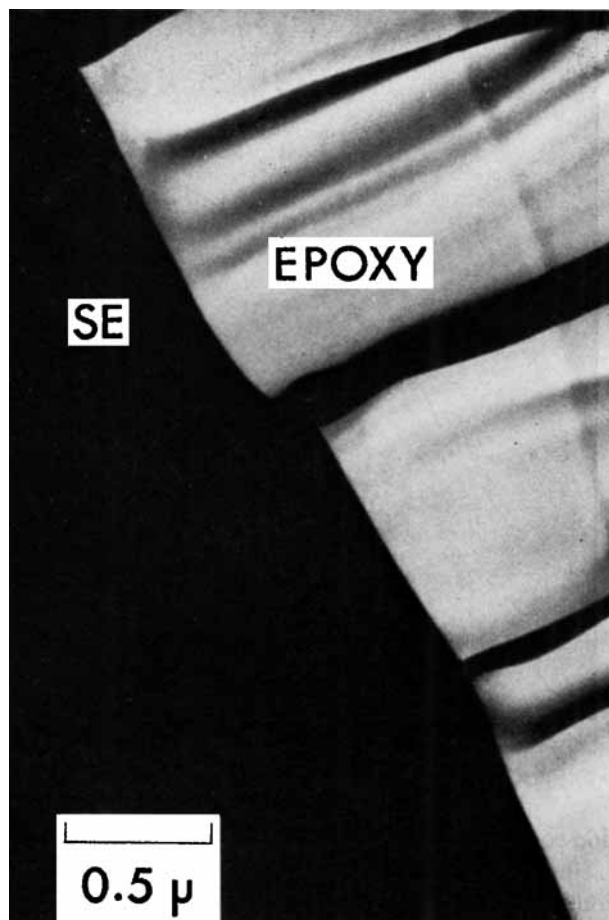


Fig. 3. Transmission electron micrograph of ultrathin sections of Se-epoxy interface (system B).

a less well defined region where there are graded concentrations of selenium in the epoxy.

When the amount of curing agent is increased to 40 parts (40 parts Lancaster A and 60 parts Araldite 6020 epoxy resin), the interfacial structure becomes quite different. The interfacial boundary is sharp and irregularities are greatly reduced. Usually, no occlusions of either kind (Se in epoxy or epoxy in Se) are observed.

**Curing Time before Evaporation.** One would expect that allowing a shorter curing time before starting to evaporate the selenium would have an effect on the interface structure similar to decreasing the amount of curing agent. This is exactly what was observed when the curing time was decreased from 130 to 50 min.

**Using a Different Resin.** A lower viscosity, Araldite 502 resin was substituted for the Araldite 6020 resin. We observed, as expected, a deeper and more frequent penetration of selenium particles into the epoxy.

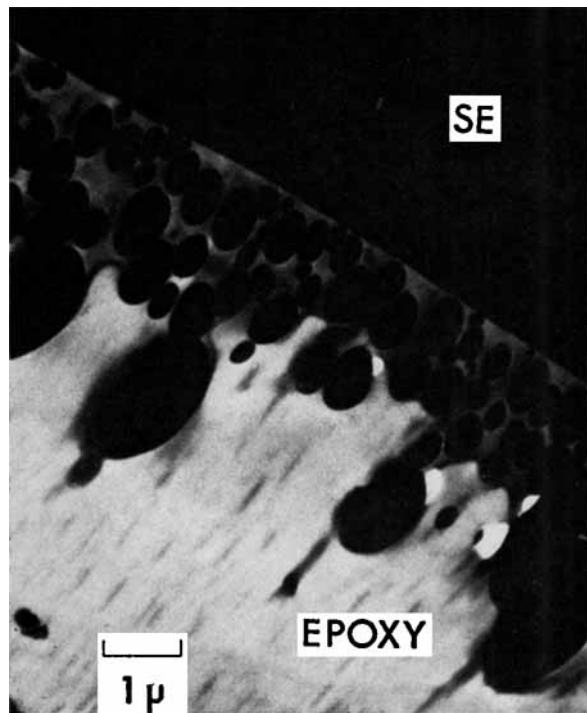


Fig. 4. Transmission electron micrograph of ultrathin sections of Se-epoxy interface (system D).

Fabrication conditions and brief descriptions of the interface layers of the systems are summarized in Table I.

As mentioned earlier, the selenium layers flaked or peeled off rather easily when selenium was deposited on well cured epoxy resin. The selenium layer detached from the cured epoxy substrate has a very smooth surface as seen from the thin cross section of it when re-embedded. And, ultrathin sectioning and electron microscopy reveals no selenium left on the separated cured epoxy layer from which the selenium layer is detached. Replicas of the separated surfaces of selenium and cured epoxy have been examined through the electron microscope. No discernible features were observed, indicating that the surfaces were very smooth. If the fracture had taken either in the bulk selenium or in the epoxy, one would expect a more irregular surface topography with the remnants of one material on the other. No such irregularities were detected.

Tensile stress studies, using an Instron Tester, again showed that for selenium on well cured epoxy the failure occurred at the Se-epoxy interface, and for selenium on incompletely cured epoxy, the failure occurred in the bulk of selenium due to fracture.

Note that, in all cases, electron diffraction showed no crystallization of selenium throughout the selenium layer.

**TABLE I**  
Summary of Interfacial Features Observed in Various Systems

Device systems designation	System description	Figure No.	Observations
System A	30 parts Lancaster A, 70 parts Araldite 6020 resin; epoxy mixture cured for 130 min before Se evaporation.	2	Penetration depth of Se into epoxy 4000 Å, epoxy into Se 7500 Å, Se particle size ~2500 Å
System B	30 parts Lancaster A, 70 parts Araldite 6020 resin; epoxy mixture cured for 16 hr before Se evaporation.	3	No penetration of Se into epoxy or epoxy into Se was noted
System C	30 parts nadic anhydride, 70 parts Araldite 6020 resin; epoxy mixture cured for 130 min before Se evaporation.		Penetration of Se into epoxy is about 7 μ, and epoxy into Se 18.5 μ <sup>a</sup>
System D	20 parts Lancaster A, 80 parts Araldite 6020 resin; epoxy mixture cured for 130 min before Se evaporation.	4	Penetration depth of Se into epoxy is about 10 μ and epoxy into Se 4.5 μ
System Dd (device 80-20-6)	20 parts Lancaster A, 80 parts Araldite 6020 resin in methyl ethyl ketone (90% ketone 10% resin mixture) used as source for depositing epoxy onto aluminum substrate; epoxy mixture cured for 130 min before Se evaporation.	7	In general, similar to system D
System E	40 parts Lancaster A, 60 parts Araldite 6020 resin; epoxy mixture cured for 130 min before Se evaporation.		Penetration depth of Se into epoxy is about 1500 Å <sup>a</sup>
System Ee (device 60-40-6)	40 parts Lancaster A, 60 parts Araldite 6020 resin in methyl ethyl ketone (90% ketone, 10% resin mixture) used as source for depositing epoxy onto aluminum substrate; epoxy mixture cured for 130 min before Se evaporation.		Penetration depth of Se into epoxy is about 1500 Å <sup>a</sup>
System F	30 parts Lancaster A, 70 parts Araldite 6020 resin; epoxy mixture cured for 50 min before Se evaporation.		Penetration depth of Se into epoxy 1.5 μ and epoxy into Se 2.9 μ, Se particle size ~1 μ
System G	30 parts Lancaster A, 70 parts Araldite 502 resin; epoxy mixture cured for 50 min before Se evaporation.		Penetration depth of Se into epoxy 2 μ and epoxy into Se 5.5 μ, Se particle size 1.4 μ

<sup>a</sup> Measured as the ridges at the interfaces.

*Photoelectric Property Characteristics*

The characteristic properties of two samples of selenium evaporated onto an incompletely cured epoxy on Al assembly were determined by xerographic measurements.<sup>3</sup> The difference between the two samples was in the epoxy layer. One sample (device Dd, 80-20-6) consisted of 20 parts Lancaster A and 80 parts resin. The second sample (device Ee, 60-40-6) consisted of 40 parts Lancaster A and 60 parts resin. The thickness of the epoxy layer was in the neighborhood of  $2 \mu$  ( $\pm 0.25 \mu$ ) for device Ee and approximately  $3 \mu$  ( $\pm 0.5 \mu$ ) for device Dd. The photoresponses of the Se-epoxy-Al plates were compared with that of a standard selenium plate (Se evaporated onto thermally oxidized aluminum at  $50^\circ\text{C}$ ). The selenium on the standard plate was  $27 \mu$  thick and on devices Dd and Ee,  $26.2 \mu$  thick. The photoconductor films were dark charged to an initial field of around  $3 \times 10^5 \text{ V/cm}$  before exposure to light.

The standard selenium exhibited no residual potential for positive surface charging, whereas device Dd showed a residual of  $+170 \text{ V}$  and device Ee a residual of  $+200 \text{ V}$  after photodischarging in white light. Residual poten-

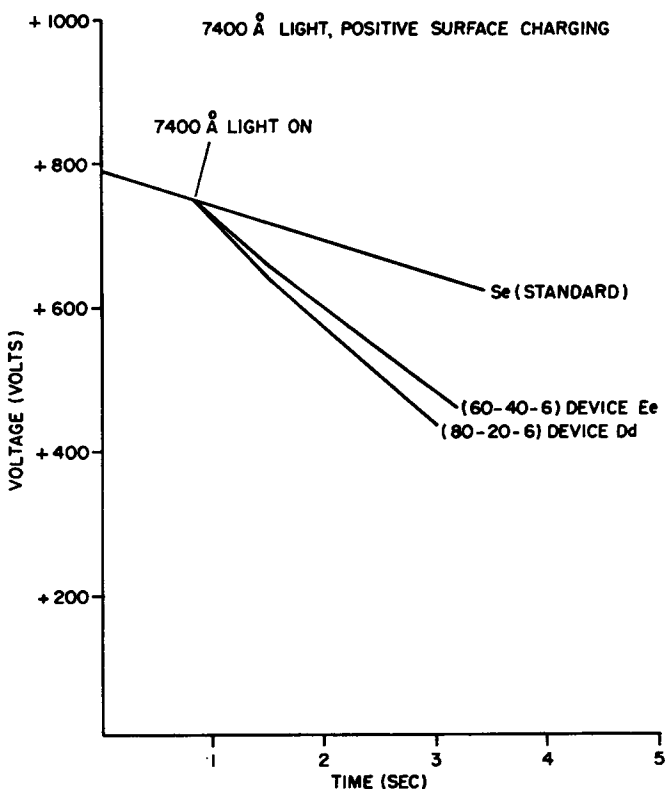


Fig. 5. Voltage decay curve of photodischarge of Se photoreceptor systems (positive surface charging).



tial is the potential difference measured with respect to ground after the device has been exposed to intense light for a long time. All the plates were dark-charged to approximately the same voltage. For negative surface charging, all three plates had the same initial photodischarge rate for light of wavelength  $4250 \text{ \AA}$ . No residual potential was observed for the standard selenium and device Dd, but a residual potential of  $-100 \text{ V}$  was observed for device Ee. Measurements of photodischarge at  $7400 \text{ \AA}$  indicate that the standard selenium plate had no detectable response for either positive or negative surface charging. Both device Dd and device Ee showed some response under illumination with wavelength  $7400 \text{ \AA}$  light. Faster discharging rates were obtained for positive surface charging than for negative surface charging with the same light intensity and device Dd was more sensitive than device Ee. The results of these measurements are plotted in Figures 5 and 6. The interfacial structure of device Ee as revealed through ultrathin sectioning and electron microscopy, showed that the selenium and the Al substrate were separated by an ordinary epoxy layer,  $2 \mu$  thick, with no selenium particles dispersed in it. On the other hand, for device Dd a continuous selenium path was observed leading from the selenium layer to the Al substrate by interconnecting selenium particles dispersed throughout the whole  $3\text{-}\mu$  epoxy layer (see Fig. 7).

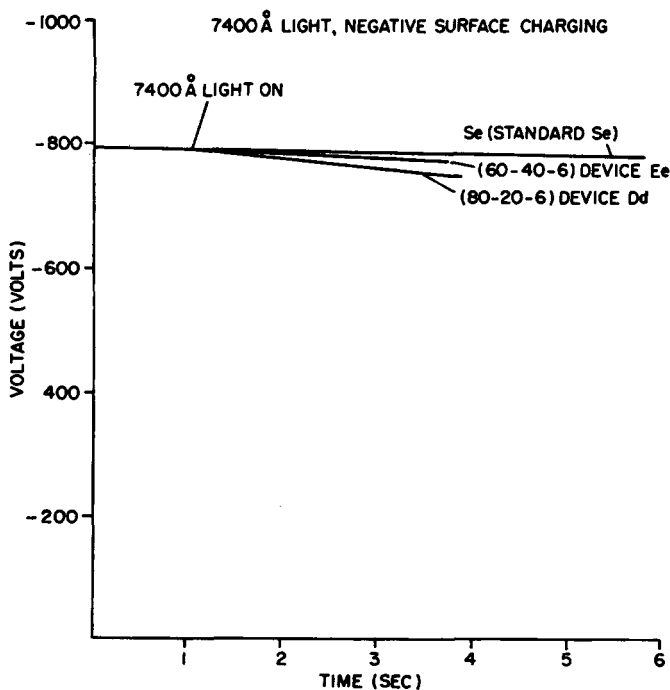


Fig. 6. Voltage decay curve of photodischarge of Se photoreceptor systems (negative surface charging).

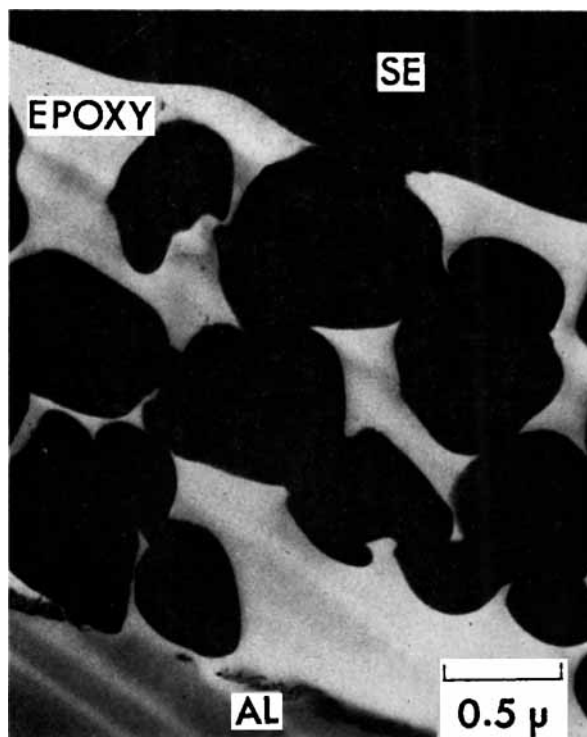


Fig. 7. Transmission electron micrograph of ultrathin sections of device Dd (System Dd).

### Selenium-Thermoplastic Resin System

Selenium was evaporated onto various types of thermoplastics having relatively low softening temperatures. Occlusion of selenium particles and dilute dispersions of selenium in the resin matrix at the interfacial region were observed in many cases (see, for example, Fig. 8). The very irregular interfacial boundaries were also observed on numerous occasions.

The Se-phenoxy resin system is closely related to the Se-epoxy resin system, in view of the similarity of the basic chemical structure of the two resins. The phenoxy resin used is the Union Carbide Bakelite phenoxy resin PAHJ with a softening temperature of 100°C. Samples fabricated at a substrate temperature of 50°C could not withstand the peeling test, and selenium was easily removed from the phenoxy resin by a piece of cellophane tape. The interfacial structure as revealed through ultrathin sectioning and electron microscopy showed a smooth junction at the selenium and the phenoxy resin interface. No penetration or occlusion of selenium in the phenoxy resin was observed. On the other hand, samples prepared at a substrate temperature of 80°C withstood the peeling test very well, the selenium layer adhered to the phenoxy resin even after repeated peelings by

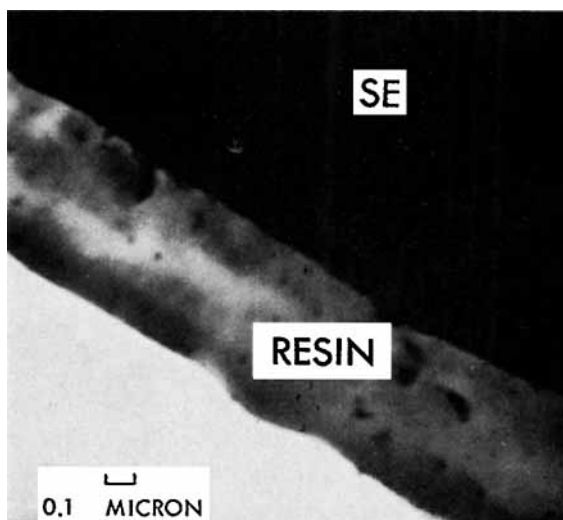


Fig. 8. Transmission electron micrograph of ultrathin sections of Se/styrene-butadiene copolymer resin interface.

using the cellophane tape. The corresponding interfacial structure showed a jagged interface and dilute dispersions of selenium in the phenoxy resin was also observed at the interfacial region.

For the Se-polyamide resin system, the resin used was that of General Mills Versalon 1112 with a softening point of 105–115°C. The selenium deposition was made at a substrate temperature of 50°C. Irregular boundaries and occlusion of selenium particles as well as dilute dispersions of selenium in the resin matrix were noted along parts of the interface but not along the other parts of the Se-polyamide junction. Selenium could easily be detached from the polyamide, for example, by peeling with a piece of cellophane tape in places where there was no apparent interaction of the resin with the selenium at the interfacial region. However, at those parts where occlusion of selenium particles and dispersions of selenium in the resin have occurred, the selenium film adhered firmly to the polyamide layer.

Experiments with selenium and the low softening point copolymer resin systems included the resin of Goodyear Pliolite S5D, VT, AC, and VTAC with the respective softening points of  $50 \pm 3$ ,  $48 \pm 3$ ,  $55 \pm 3$ , and  $53.5 \pm 3$ °C. Two substrate temperatures, 0 and 50°C, were used. It was observed that penetration of selenium into the various copolymer resins was much deeper and the interface more irregular for films evaporated at higher substrate temperature than at the lower substrate temperature.

The polyethylene used in the Se-polyethylene system was the Borden Chemical's Monomer-Polymer Laboratories high-density polyethylene (melting point approximately 138°C). The polyethylene film was an oriented partially crystallized layer as seen from the ultrathin cross sections

of the system under the electron microscope. The interface of the Se-polyethylene gave an irregular and diffused boundary between the two materials. Dilute dispersions of selenium in the polyethylene matrix together with some occluded selenium particles were seen. The selenium could easily be peeled off the metal substrate by using a cellophane tape. Cross-section studies revealed that the failure occurred mainly in the polyethylene and not at the interface. The thickness of the polyethylene layer on selenium after peeling off the aluminum foil was generally in the range of 2000–4000 Å.

## DISCUSSION

When selenium was evaporated onto well cured epoxy resins, even after the epoxy surface was treated by helium ion bombardment\* under reduced pressure, the resulting bond was relatively weak and would fail under flexing or stripping. This is associated with the interface structure shown in Figure 3, i.e., a very smooth junction. No irregularities at the interface or occlusion of selenium in epoxy is seen. The cross section and the replication studies indicate that the separation occurs right at, or in the extremely close vicinity of, the interface. These observations suggest the interface is the weakest link of the structure.

In contrast, selenium evaporated onto incompletely cured epoxy resin resulted in a strong bond and easily withstood the stress of flexing or stripping. The interfacial structures in such cases (see Figs. 2 and 4) characteristically show interpenetration of selenium and epoxy forming jagged interfaces. In most cases, the dispersions of one phase in the other in the form of particles are also apparent. Further, the electron micrograph (Fig. 4) indicates the occurrence of gross mixing and molecular diffusion of selenium into the epoxy resin in the interfacial region. Similarly, the molecular diffusion of epoxy into selenium can also be surmised. The latter is not evident from the electron micrographs because a small concentration of a low-density material in a high-density matrix does not give enough contrast to be differentiated.

We conclude that the much improved adhesion of selenium deposited on incompletely cured epoxy compared to the adhesion of selenium deposited on well cured epoxy can be attributed to (1) the gross intermixing and molecular interdiffusion of the materials in the interfacial region and (2) the mechanical interlocking of the irregularities at the interface. The latter, however, are introduced in many cases as a result of the former. Krotova and Movozova<sup>6</sup> have attributed the adhesion of polymers to a diffusion process in the contact region, as proposed earlier by Voyutskii et al.,<sup>7,8</sup> and have shown by the luminescence method that this interdiffusion process occurs.

\* Inert gas ion (i.e., helium, argon, etc.) bombardment of polymer surfaces have been reported to increase the strength of adhesive joints by eliminating the "weak layers" presented on the surface; for details see Hansen and Schonhorn.<sup>4,5</sup>

It is also important to point out that the penetration of selenium particles into the epoxy layer, as seen in the various figures, is not caused by gravity, since during evaporation of the selenium the epoxy layer surface was facing downward. Further, it has been demonstrated that the above mentioned features were amplified by using lower viscosity resin mixtures such as slower acting curing agents, shorter curing time before selenium evaporation, and by reducing the amount of curing agents used. As expected, these migration, mixing, and molecular diffusion processes proceed faster in a less viscous medium.

There is a very close relationship between the penetration depth of the selenium particles into the epoxy resin and the size of the selenium particles themselves. For example, the particle size of selenium in Figure 2 is almost 2500 Å, and the penetration depth is 4000 Å. In Figure 4, the particle size is about 5  $\mu$  and the penetration depth is 10  $\mu$ . For system F (see Table I), the particle size is 1  $\mu$  and the penetration depth is 1.5  $\mu$ , while for system G the particle size is 1.4  $\mu$  and the penetration depth is 2  $\mu$ .

From the variation of selenium particle size with depth of penetration together with the shape of some of the particles (some of them seen in Fig. 4), it seems rather evident that coalescence of these selenium particles took place. Interdiffusion of selenium into the epoxy resin between the spaces separating the individual selenium particles can be seen in Figure 4. Thus, when selenium is evaporated onto a very thin and incompletely cured epoxy resin, a Se-epoxy binder layer is actually formed between the selenium bulk and the metallic substrate (see Figure 7).

By drawing analogies with a large number of other semiconductor-organic resin binder layers,<sup>2</sup> we expect the Se-dispersed-in-epoxy system to be electrically conductive, but the range of the electron and the hole could be drastically different in this composite material. Xerographic measurements confirmed this by showing that for negative surface charging, the system corresponding to Figure 7, system Dd, has no residual potential after photodischarging. Apparently, the selenium binder layer allowed easy transit of electrons. For system Ee, in which the selenium penetration into the epoxy was small, a residual potential of -100 V was obtained. Postulating complete photodischarge in the selenium layer and taking a dielectric constant of 3.6 for the epoxy,<sup>9</sup> we calculated a residual potential of -90 ( $\pm 11$ ) V for a perfectly insulating epoxy interface layer 2 $\mu$  ( $\pm 0.25\mu$ ) thick. The close correspondence between the calculated and the measured residual potential indicates that, upon photodischarge, the electrons are mostly trapped at the Se-epoxy interface. However, it appears that discharge across the epoxy layer can still occur as the electric field exceeds  $5 \times 10^5$  V/cm, since repeated charging and discharging of the photoconductor showed no substantial alteration of the residual potential.

For positive surface charging, both devices exhibited residual potentials after photodischarge in white light: 170 V for system Dd and 220 V for system Ee. We believe that these residual potentials are partially due to hole trapping in the selenium layer adjacent to the epoxy since these volt-

ages exceed the values calculated for complete discharge of the selenium. Ing and Chiang<sup>10</sup> have doped selenium with various organic donor molecules and have shown these selenium materials to contain hole trapping centers. The epoxy systems used consisted of strong donors, such as the polyamines, and are likely to have diffused into the selenium layer; thus, the selenium becomes donor-doped. Ing and Chiang also discovered that organic-donor-doped selenium shows extrinsic photoconductivity in the long wavelength region (peaks around 7400 Å) of the light spectrum. For devices Dd and Ee, the long wavelength responses were indeed observed (see Figs. 5 and 6) in contrast to the standard selenium which showed no response at 7400 Å. These observed responses were not due to crystallized selenium, since no crystallization could be detected in any case. The voltage decay rates upon photoexcitation using 7400 Å light are substantially higher for positive than for negative surface charging, and for negative charging, the photoresponses were very small. This is consistent with the suggestion that 7400 Å donor doping is confined to a thin selenium layer next to the epoxy. The 7400 Å light is highly penetrating, with an absorption coefficient of around  $30 \text{ cm}^{-1}$  in amorphous selenium,<sup>11</sup> and thus can give rise to extrinsic photoconductivity in the doped Se layer. It is likely that electrons are released from the donor centers to the conduction band. For positive surface charging, the freed electrons can migrate to the selenium free surface, thus discharging the photoconductor. For negative surface charging, the electrons move toward the epoxy layer and, in the case of device Dd, the electrons are able to transit across the Se-epoxy interface. This is equivalent to displacing the virtual anode towards the negatively charged selenium surface, thus lowering the plate potential.

The electrical measurements made of these photoconductor systems were not exhaustive but have been very useful in characterizing these device structures. Furthermore, the results have been extremely helpful in substantiating some of the important conclusions we have reached through the electron microscopy examination of the selenium structures.

As mentioned earlier, the results on the other Se-organic resin systems were quite similar to that of the Se-epoxy system. The gross intermixing and molecular interdiffusion of the materials in the interfacial region have been observed in many cases, and are related to the mechanical bonding characteristics of the composite system. These results lend further support to the conclusions presented in this paper.

### References

1. R. Houwink and G. Salomon, *Adhesion and Adhesives*, 2nd Ed., Elsevier, New York, Vol. 1, 1965, Vol. 2, 1967.
2. J. Dessauer and H. Clark, *Xerography and Related Processes*, Focal Press, New York, 1965.
3. H. J. Gerritsen, W. Ruppel, and A. Rose, *Helv. Phys. Acta.*, **30**, 504 (1957).
4. R. H. Hansen and H. Schonhorn, *J. Polym. Sci. B*, **4**, 203 (1966).
5. H. Schonhorn and R. H. Hansen, *J. Appl. Polym. Sci.*, **11**, 1461 (1967).

6. N. A. Krotova and L. P. Movozova, *Dokl. Akad. Nauk SSSR*, **127**, 141 (1959).
7. S. S. Voyutskii, A. I. Shapovalova, and A. P. Pisarenko, *Dokl. Akad. Nauk SSSR* **105**, 1000 (1955).
8. S. S. Voyutskii, *Vysokomol. Soedin.*, **1**, 230 (1959).
9. Ciba Products Corporation Technical Bulletin *Lancast A*, No. 11121/3, Fairlawn, New Jersey.
10. S. W. Ing and Y. S. Chiang, paper presented at the 153rd American Chemical Society Meeting, Miami Beach, April 1967.
11. J. L. Hartke and P. J. Regensburger, *Phys. Rev.*, **139**, A970 (1965).

Received June 10, 1968

Revised August 23, 1968